

Deformation and strength anisotropy of calcareous slates under Brazilian tests

Mohammad Hosein Ghobadi^{*1}, Paria Behzadtabar²;

1 & 2. Department of Geology, Bu-Ali Sina University

Received: 11 Aug 2016

Accepted: 15 Feb 2017

Abstract

Rock anisotropy plays an important role in engineering behavior of rocks. Slates are anisotropic rocks which have long been used for gable roof, floor tiles, borrow materials, and other purposes. The slates studied in this research are calcareous and have a porphyro-lepidoblastic texture. To determine the role of the anisotropy on the tensile strength and fracture pattern, two variables including ψ (the core axis angle to foliation) and β (the angle between the axis of loading and foliation) in the Brazilian tests were used. The angles were selected at 15° intervals. Thus, for both ψ and β , seven angles of 0° , 15° , 30° , 45° , 60° , 75° , and 90° were selected (i.e., there are 43 possible modes). In order to name and examine the failure pattern, 11 models were proposed. The average value of the failure strength for the three stations varies from 3.21 MPa to 20.94 MPa. Based on the obtained results, there is a direct relation between the average tensile strength and density. A comparison between Brazilian test data under dry and saturation conditions shows that the saturated Brazilian tensile strength is 30.8% less than the dry Brazilian tensile strength. Moreover, the changes in fracture length with the

^{*}Corresponding Author: amirghobadi@yahoo.com

changes in ψ and β indicate an inverse relation. Eventually, the average of tensile strength (σ_t) and strength anisotropy index (I_a) demonstrates that the influence of orientation angle (ψ) is much larger than that of foliation-loading angle (β).

Keywords: Anisotropy, Slate, Brazilian test, Fracture pattern, Tensile strength

Introduction

An anisotropic rock has different properties in different directions. These properties may be of any type such as deformability modulus, strength, brittleness, permeability, and discontinuity frequency (Hudson and Harrison 1997).

Rock anisotropy plays an important role in various engineering activities, such as stability of underground excavations, surface excavations, foundations, drilling, blasting, rock cutting, directional fluid flow, and contaminant transport (Chen et al. 1998).

In recent investigations, different techniques and methods have been developed to determine geotechnical properties of anisotropic rocks. Uniaxial and triaxial compression, punching, point load, and Brazilian tests are the most important laboratory tests for studying geotechnical properties of anisotropic rocks. Theoretical and laboratory studies to estimate the strength, failure shape, and deformation properties of anisotropic rocks have been undertaken by many researchers (Khanlari et al. 2014; Ikari et al. 2015; Heng et al. 2015; Shuai et al. 2015; Cho et al. 2012; Debecker and Vervoort 2013; Yilmaz and Yucel 2014; Vervoort et al. 2014; Park and Min 2015; Duan and Kwok 2015; Nasser et al.

1997; Stoeckhert et al. 2015; Saeidi et al. 2014; Zhong et al. 2015; Islam and Skalle 2013; Ajalloeian and Lashkaripour 2000; Dan et al. 2013; Tavallali and Vervoort 2013).

Tensile strength is an important parameter for determining the load bearing capacity of rocks, deformations, damage, or fracturing. This parameter is used to analyze the stability and serviceability of rock structures. In this regard, some studies have been conducted to estimate the tensile strength of anisotropic rocks by Brazilian test (Duan and Kwok 2015; Vervoort et al. 2014; Khanlari et al. 2014; Tavallali and Vervoort 2013).

This research was conducted to determine the effect of the orientation on both the tensile strength and the failure pattern of calcareous slate in Brazilian test. Furthermore, in order to investigate the role of water in Brazilian test results, 21 samples ($\psi=0^\circ$) each per a station (in total 63 samples for all three stations) were saturated and then tested under saturated condition.

Experimental method

Brazilian test

Brazilian test (or indirect tensile strength test) is the most common testing procedure for the determination of the maximum tensile failure strength (σ_t). In this test, a disk-shaped rock specimen is subjected to a uniaxial compression loading. The Brazilian tensile strength (σ_t)

perpendicular to the loaded diameter, based on linear elastic calculations, can be written as:

$$\sigma_t = \frac{2P}{\pi Dt} \quad (1)$$

where P is the applied load (at the moment of failure) and D and t are the diameter and the thickness of the disc-shaped samples, respectively.

Specimen preparation

In general, the preparation of the test specimens, their dimensions, and the minimum number of test specimens are necessary to determine the properties of anisotropic rocks based on the applied method (Chen et al. 1998). The International Society of Rock Mechanics (ISRM, 2007) and ASTM-D-3967 suggest a method to determine the tensile strength of rock materials. For the purpose of this study, slate blocks of three stations (N, M, and G) were chosen. Then, the Brazilian tests were carried out according to ISRM (2007) recommendations on cylindrical samples with diameter D=54 mm and height to diameter ratio h/D=0.5. The sampling process for the specimens prepared for the Brazilian tests is illustrated in Figure 1. Seven different values were considered for ψ (the core axis angle to foliation) and β (the angle between the axis of loading and foliation) parameters: 0°, 15°, 30°, 45°, 60°, 75° and 90°. For each orientation, 2 to 3 samples were tested. By changing ψ and β at 15° intervals, 43 possible states were created.

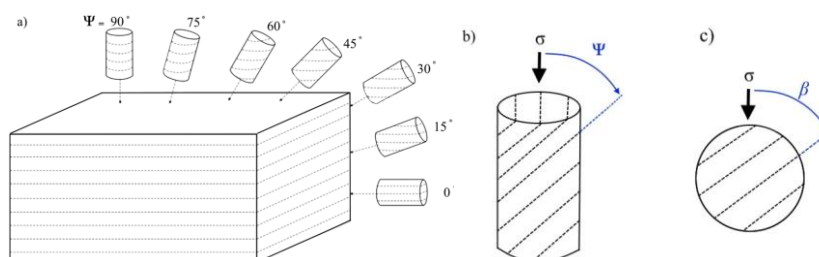


Figure 1. a) Directional coring diagram of specimens with different bedding orientations, b) Directional coring (ψ) for slate sample preparation, c) Loading angle relative to the surface anisotropy (β) in Brazilian test

Material properties

Petrography (thin section and XRD) and physical properties

Diamantis et al. (2014) demonstrate that the physicommechanical characteristics are strongly influenced by the petrographical characteristics except for mineral grain size.

The thin sections and XRD¹ test results are presented in Table 1. Platy minerals such as muscovite, basically consisting of extended flat sheets of linked silicates, display flat or flaky crystal habit or planar cleavage. The presence of pyrite in these slates leads to the generation of a porphyritic texture. In some slates, it is also possible to find limestone fragments (Cárdenes et al. 2010) such as those found in the samples studied.

Physical properties of the rock samples, such as dry and saturated unit weights (γ_d , γ_{sat} , and γ_{sub}), specific gravity (G_s), porosity (n), and water absorption (W_a) were determined using the standard testing

¹ X-ray Diffraction

procedure suggested by ISRM (2007). For this purpose, five sets of tests were performed on the core specimens prepared in two directions of anisotropy planes (β is 0° and 90°). Hence, a total of 30 tests was performed for calculating physical properties (Table 2).

Table 1. Mineral composition of tested samples

Station	Rock type	Fabric	Mineral content ^a
N	Calcareous slate	Porphyro-lepidoblastic	Cal, Qtz, Mic, Pry, Hem, Gr
M	Calcareous slate	Porphyro-lepidoblastic	Cal, Qtz, Plg, Mus, Pry, Hem, Gr
G	Calcareous slate	Porphyro-microgranular Microgranular	Cal, Qtz, Fld, Mus, chl, Hem, Gr

^a:Qtz.: Quartz, Mic.: Mica, Fld.: Feldspar, Mus.: Muscovite, Chl.: Chlorite, Gr.: Graphite, Hem.: Hematite, Pyr.: pyrite, Plg.: Plagioclase.

Table 2. Physical properties of samples

Station	γ_d (gr/cm ³)	γ_{sat} (gr/cm ³)	γ_{sub} (gr/cm ³)	G _s	n (%)	Wa (%)
N	2.86	2.87	1.86	2.92	2.21	0.82
M	2.78	2.8	1.75	2.84	2.2	0.81
G	2.87	2.86	1.81	2.89	0.71	0.26

As given in Table 2, the dry unit weight ranges between 2.78 g/cm³ and 2.87 g/cm³ with an average of 2.83 g/cm³; the porosity ranges between 0.71% and 2.21% with an average of 1.70%; and the water absorption ranges between 0.26% and 0.82% with an average of 0.63%.

According to the classification of dry density and porosity (Anon 1974), the porosity of samples falls in classes 4 and 5 (low and very low) while density falls in class 5 (very high). An interesting observation is that water absorption in the samples with $\psi = 0^\circ$ is greater than those with $\psi = 90^\circ$. This remark is explainable by the larger number of weakness planes in these specimens and the capillary effect of vertical joints.

Discussion

Tensile strength values

Siegesmund and Dürrast (2011) noted that one of the main factors affecting the tensile strength is the existence and spatial orientation of any foliation or sedimentary layering in the rock sample and the loading direction in respect to these rock fabric elements.

The orientation of the sample in relation to the loading direction is important in anisotropic materials as it controls the peak strength. Tensile strength values obtained with a different orientation (ψ) and foliation-loading (β) angles are presented in Tables 3 and Figure 2. In general, with an increase in ψ (0° to 90°), the minimum σ_t values are observed at higher β , except for sample extracted in station N. For other samples for $\psi < 45^\circ$, the maximum σ_t is observed at $\beta > 45^\circ$ while for $\psi > 45^\circ$ the maximum σ_t is observed at $\beta < 45^\circ$. Based on the samples studied, it is clear that the influence of ψ on tensile strength is more than that of in β . Dan and et al. (2013) indicated that the influence on the determined peak strength of ψ is much stronger than that of β . Strohmeyer and Siegesmund (2002) found a variation of the tensile strength values, from 7 MPa to 14 MPa, related to the differences in rock fabrics for a metagabbro from Anzola, with hornblendes showing a perfect cleavage.

The Brazilian anisotropy index is a proper index for anisotropic rocks. This index is defined as the ratio of σ_t values for each ψ or each β , measured in the strongest and weakest directions ($I_a = \sigma_{t(\max)} / \sigma_{t(\min)}$).

Table 3. Results of Brazilian tensile strength and Brazilian anisotropy index (Ia): a) Station N, b) Station M, and c) Station G.

a)	$\psi=0^\circ$	$\psi=15^\circ$	$\psi=30^\circ$	$\psi=45^\circ$	$\psi=60^\circ$	$\psi=75^\circ$	$\psi=90^\circ$	Ia(β)
$\beta=0^\circ$	7.78	4.48	11.36	12.97	13.48	10.24	15.44	3.44
$\beta=15^\circ$	8	9.48	3.56	13.28	12.11	12.43	-	4.33
$\beta=30^\circ$	9.21	7.79	10.19	7.74	13.97	12.43	-	1.99
$\beta=45^\circ$	9.43	16.24	7.08	15.10	6.59	19.81	-	3.00
$\beta=60^\circ$	10.30	5.12	4.00	9.17	8.95	9.16	-	3.86
$\beta=75^\circ$	10.59	6.31	3.66	14.63	11.38	10.52	-	4.21
$\beta=90^\circ$	13.45	10.29	7.85	17.25	8.23	10.10	-	2.19
Ia(ψ)	1.72	3.62	3.19	2.22	2.11	2.16	1	

b)	$\psi=0^\circ$	$\psi=15^\circ$	$\psi=30^\circ$	$\psi=45^\circ$	$\psi=60^\circ$	$\psi=75^\circ$	$\psi=90^\circ$	Ia(β)
$\beta=0^\circ$	6.68	7.48	3.93	12.81	11.18	20.7	12.66	5.27
$\beta=15^\circ$	5.85	5.44	5.46	12.79	16.75	18.12	-	3.33
$\beta=30^\circ$	7.19	6.83	2.27	11.52	15.54	18.92	-	8.33
$\beta=45^\circ$	7.97	6.98	3.19	8.81	11.54	17.97	-	5.63
$\beta=60^\circ$	9.31	8.13	4.25	9.26	14.40	20.69	-	4.87
$\beta=75^\circ$	12.66	8.93	9.35	13.82	13.59	18.72	-	2.10
$\beta=90^\circ$	10.21	10.59	13.28	11.04	10.89	15.80	-	1.55
Ia(ψ)	2.16	1.95	5.85	1.57	1.54	1.31	1	

c)	$\psi=0^\circ$	$\psi=15^\circ$	$\psi=30^\circ$	$\psi=45^\circ$	$\psi=60^\circ$	$\psi=75^\circ$	$\psi=90^\circ$	Ia(β)
$\beta=0^\circ$	6.51	7.67	12.51	12.19	13.31	17.93	21.42	3.29
$\beta=15^\circ$	3.80	9.78	16.33	13.09	17.84	16.63	-	5.64
$\beta=30^\circ$	10.37	9.44	13.45	22.32	10.24	17.12	-	2.36
$\beta=45^\circ$	6.19	9.38	11.12	10.72	10.66	18.97	-	3.46
$\beta=60^\circ$	5.42	14.78	16.88	11.39	10.24	16.88	-	3.95
$\beta=75^\circ$	16.87	9.73	17.53	7.98	9.98	14.30	-	2.68
$\beta=90^\circ$	18.92	9.76	18.32	7.69	4.20	17.76	-	5.10
Ia(ψ)	4.98	1.93	1.65	2.90	4.25	1.33	1	

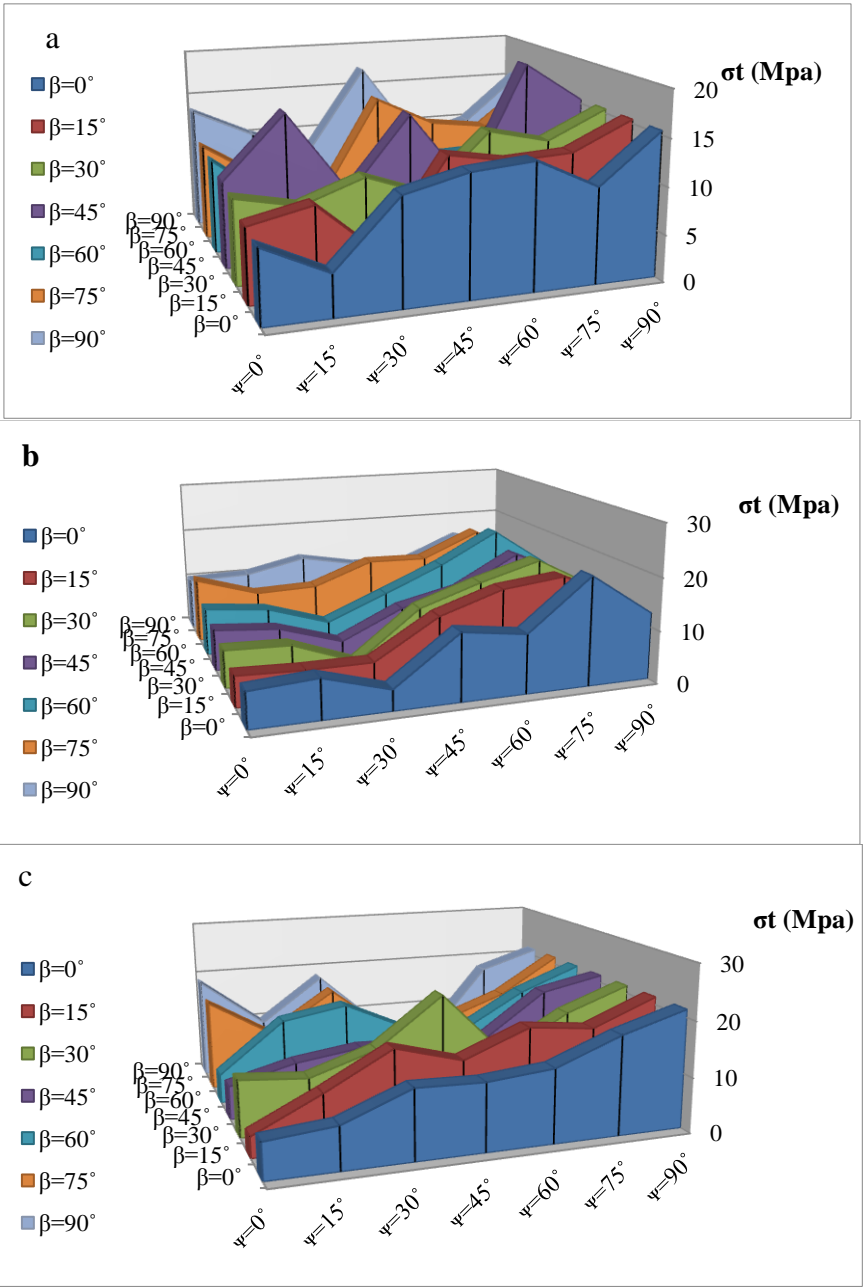


Figure 2. Results of Brazilian tensile strength: a) Station N, b) Station M, c) Station G.

Because of the absence of strongest and weakest directions (foliation), Brazilian anisotropy index (I_a) is close to 1.0 for isotropic rocks and is at higher values for anisotropic rocks.

In this respect, based on the relationship between the average minimum tensile strength of the Brazilian ($\sigma_{t \text{ (min. av)}}$), physical properties (n and γ_d), and average Brazilian anisotropy index ($I_{a \text{ (}\psi \text{. AV)}}$ and $I_{a \text{ (}\beta \text{. av)}}$), the best equations were presented in Table (4).

Table 4. Linear regression between physical properties, tensile strength, and anisotropy index

Eq.	Correlation Coefficient (R)	N.
$\sigma_{t \text{ (min.av)}} = 0.0587\gamma_d + 2.6489$	0.998	2
$I_{a \text{ (}\psi \text{.av)}} = 3.8219\gamma_d - 8.4672$	0.755	3
$I_{a \text{ (}\psi \text{.av)}} = -0.2834n + 2.858$	0.973	4
$I_{a \text{ (}\beta \text{.av)}} = -10.034\gamma_d + 32.3$	0.857	5
$I_{a \text{ (}\beta = i)} = 0.37I_{a \text{ (}\psi = i)}^3 - 3.5I_{a \text{ (}\psi = i)}^2 + 10.11I_{a \text{ (}\psi = i)} - 5$	0.77	6

* σ_t :Mpa γ_d : g/cm³, n:%, ψ and β : degree

A comparison between $I_{a \text{ (}\psi)}$ and $I_{a \text{ (}\beta)}$ reveals that $I_{a \text{ (}\psi)}$ is less than $I_{a \text{ (}\beta)}$, suggesting that the Brazilian anisotropy index is more sensitive to the changes in ψ than those of β .

The impact of saturation conditions on the Brazilian tensile strength ($\psi=0^\circ$)

Water in rocks increases pore water pressure and reacts with minerals. These effects are particularly seen in heterogeneous and porous rocks. In slates, water shows its role majorly through the foliation, joints, and veins. To examine water role in slate, 21 samples from each station (63 samples) with $\psi=0^\circ$ were prepared and immersed in water for 48 h. Next, samples were tested at 7 different angles. As shown in Figure 3, Brazilian tensile strengths show a

positive linear relation with these angles in both dry and saturated conditions.

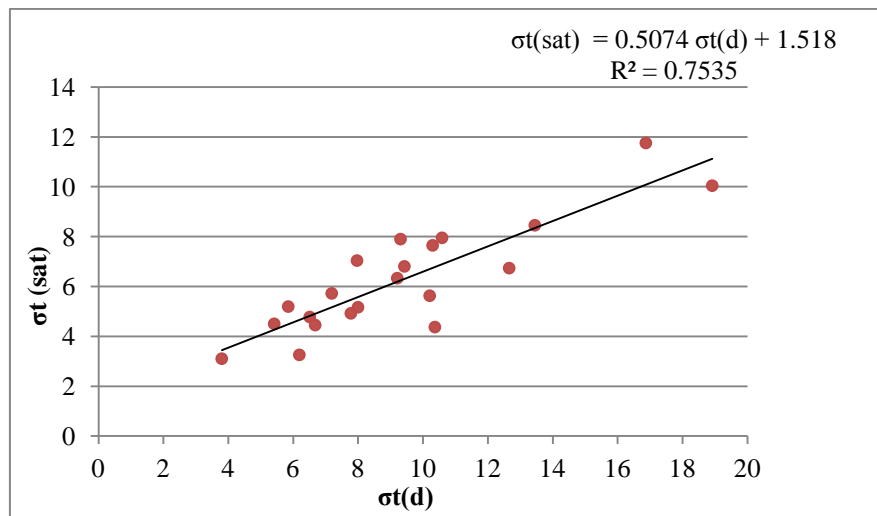


Figure 3. The relation between Brazilian tensile strength in the dry and saturation states ($\psi=0^\circ$).

To better understand these changes, the values of $\sigma_t(sat)$ with β and $\sigma_t(d)$ were plotted using Surfer 9 software package and Kriging interpolation method (Figure 4). Despite the low porosity of samples, a significant reduction was achieved. Besides, rock samples were considerably strengthened by the metamorphism, their porosity was lowered, and their permeability became virtually zero. These properties explain the suitability of slates for roofing purposes and also for sea defense walls (Smith 1999).

To demonstrate strength reduction, the strength reduction factor (RF) was used

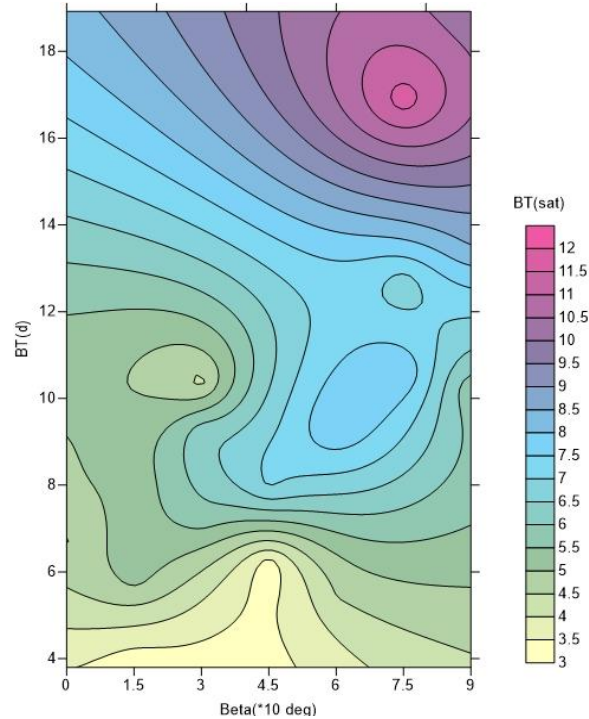


Figure 4. Kriging interpolation results for $\sigma_{t(sat)}$ using Surfer 9 software with dry Brazilian tensile strength ($BT_{(d)}$) and beta (β°) values.

$$RF_{(\beta=i)} = \frac{\left[\frac{\sum \sigma_{t(d)} - \sigma_{t(sat)}}{\sigma_{t(d)}} \right]}{N} * 100 \quad (7)$$

Where RF (β) is reduction factor, $\sigma_{t(d)}$ is the dry tensile strength, $\sigma_{t(sat)}$ is saturation tensile strength, and N is the number of samples.

The results show that Brazilian tensile strength of saturated samples is 30.8% less than that of dry samples. Yavuz et al. (2015), studied the influence of the water saturation on the strength of volcanic tuffs and reported that uniaxial compression strength (UCS) in saturated conditions (immersed for 1 h) indicates a 31.96 % decrease in UCS. They also showed that after immersing the specimens in water for 48 h, the UCS values decreases by 43.99%.

Table 5. Reduction factor of tensile strength ($\Psi=0^\circ$)

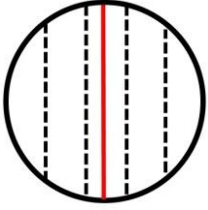
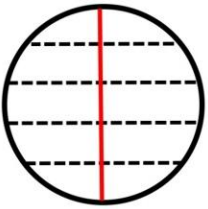
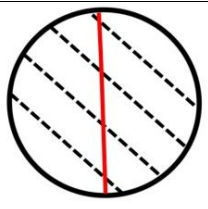
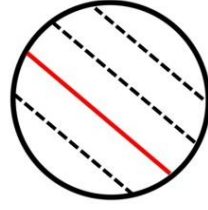
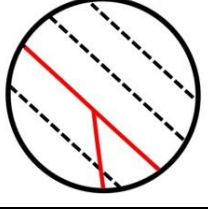
	RF (%)							
β°	$0^\circ\beta=$	$15^\circ\beta=$	$30^\circ\beta=$	$45^\circ\beta=$	$60^\circ\beta=$	$75^\circ\beta=$	$90^\circ\beta=$	AV.
N.	36.76	35.45	31.27	27.86	25.77	24.94	37.16	31.31
M.	33.41	11.26	20.44	11.72	15.17	46.81	44.88	26.24
G	26.73	18.43	57.87	47.45	16.92	30.34	46.92	34.95
RF(Av.)	32.30	21.71	36.53	29.014	19.29	34.037	42.99	30.84

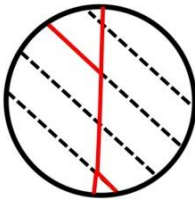
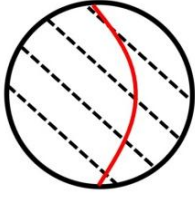
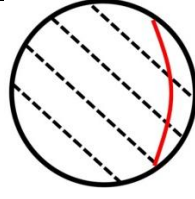
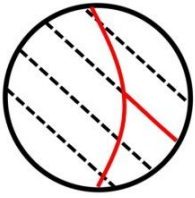
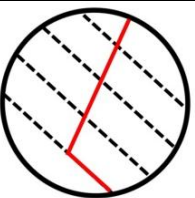
Fracture patterns

The geometry of tension cracks and fractures in relation to the pre-existing rock fabric (e.g., intergranular cracks along grain boundaries and along the rock-forming minerals) were studied by Siegesmund and Dürrast, (2011). Tavallali and Vervoort (2013), considering the post-failure behavior of anisotropic sandstone samples, defined different types of fractures: 1) Layer activation; 2) Central fractures; and 3) Non-central fractures. Based on fracture patterns observed in all samples, 10 fracture patterns (Table 6) were presented. Using this table, fractures in the samples were identified and named (Table 7).

For $\beta=0^\circ$, L and LC fracture patterns are dominant. In this case, the tensile failure in the foliation is along the loading direction; thus, in terms of tensile strength, it has the least value. For $\psi=30^\circ$, the fracture pattern is changed and both shear and tensile failure are seen as a combination (e.g., patterns of LF and FL). This trend continues until $\psi=60^\circ$. Isotropic materials show distinct tensile cracks along the centerline in contrast to anisotropic materials, where the fracture pattern is more complicated and is composed of mixed-mode cracks along the weak planes and the matrix (Dan et al. 2013).

Table 6. Fracture patterns observed in all samples based on the direction of loading and foliation (the non-continuous line is foliation and the continuous line is fracture).

Pattern	Description	Symbol
	Fracture in the direction of loading (sometimes with small deviation less than 15° to loading direction)	L
		
		
	Fracture in the direction of foliation	F
	Fracture in the direction of foliation is dominant to the fracture in the direction of loading	FL

Pattern	Description	Symbol
	Fracture to loading axis is dominant on foliation fracture. (Unidirectional fracture or Bidirectional fracture)	LF
	Curved fracture in direction of loading (curvature of fracture <1/2 radius from sample's center)	LC
	Fracture in direction of loading, but away from 1/2 radius from sample's center (off-loading)	OL
	Curved fracture in direction of loading+ fracture in direction of foliation	LCF
	Deviation of loading (probably associated with fractures to foliation)	DL

It can be concluded that the greatest effects of β occur at $15^\circ < \psi < 75^\circ$. Considering β as constant and ψ as the variable, the fracture pattern indicates a wide variety. Hence, it can be concluded

that, like tensile strength, the changes in fracture pattern is a function of ψ rather than β .

Table 7. Fracture patterns: a) Station N, b) Station M, and c) Station G.

a)	$\Psi=0^\circ$	$\Psi=15^\circ$	$\Psi=30^\circ$	$\Psi=45^\circ$	$\Psi=60^\circ$	$\Psi=75^\circ$	$\Psi=90^\circ$
$\beta=0^\circ$	L	L	L	LC	LC	L	L LC
$\beta=15^\circ$	L	L	DL	LC	LC	DL	
$\beta=30^\circ$	LF	LC	L	LF	LC	LC	
$\beta=45^\circ$	LC	LC	L	LC	L	OL	
$\beta=60^\circ$	LC	DLF	DL	LC	L	L	
$\beta=75^\circ$	LC	L LC	LD LC	LC	L	L	
$\beta=90^\circ$	LC	L LC	L DL	LF	L	L	

b)	$\Psi=0^\circ$	$\Psi=15^\circ$	$\Psi=30^\circ$	$\Psi=45^\circ$	$\Psi=60^\circ$	$\Psi=75^\circ$	$\Psi=90^\circ$
$\beta=0^\circ$	L	L	L	LC DL	LC	L	L
$\beta=15^\circ$	L	LC	LF	L OL	LF	L	
$\beta=30^\circ$	LC	FL	FL	LC	LF	L	
$\beta=45^\circ$	LC	LC	FL	LF	OL	LC	
$\beta=60^\circ$	LC	LCF	FL	OL	LCF	LC	
$\beta=75^\circ$	LCF	LF FL	FL	LCF	LF	LC	
$\beta=90^\circ$	L LC	LCF	FL	L LC	LC	L	

c)	$\Psi=0^\circ$	$\Psi=15^\circ$	$\Psi=30^\circ$	$\Psi=45^\circ$	$\Psi=60^\circ$	$\Psi=75^\circ$	$\Psi=90^\circ$
$\beta=0^\circ$	L LC	LC	L	L OL	LC	L	LC L LF
$\beta=15^\circ$	L F	LC	LC	LF LC	LC	LC	
$\beta=30^\circ$	LF	LC	LC	L	FL	L	
$\beta=45^\circ$	LF	OL	L	OL	F	L	
$\beta=60^\circ$	F	DL	L	LCF LC	DL	L	
$\beta=75^\circ$	LCF	LF	OL	FL	DL	OL	
$\beta=90^\circ$	L	L	L	L LF	LC	LC	

A comparison with the average fracture length (LF) with $Ia_{(\beta)}$ and $Ia_{(\psi)}$ (Figure 5) reveals that the influence of orientation angle (ψ) on the Brazilian anisotropy index is much larger than that of foliation-loading angle (β) ($Ia_{(\psi)} < Ia_{(\beta)}$). In addition, the location of the maximum length of the fracture, based on the variation of β (Figure 5 a) and ψ (Figure 5 b) is different. For example, at $\psi=45^\circ$, the maximum length of the fracture is observed while at $\beta=45^\circ$ the minimum average fracture length is observed.

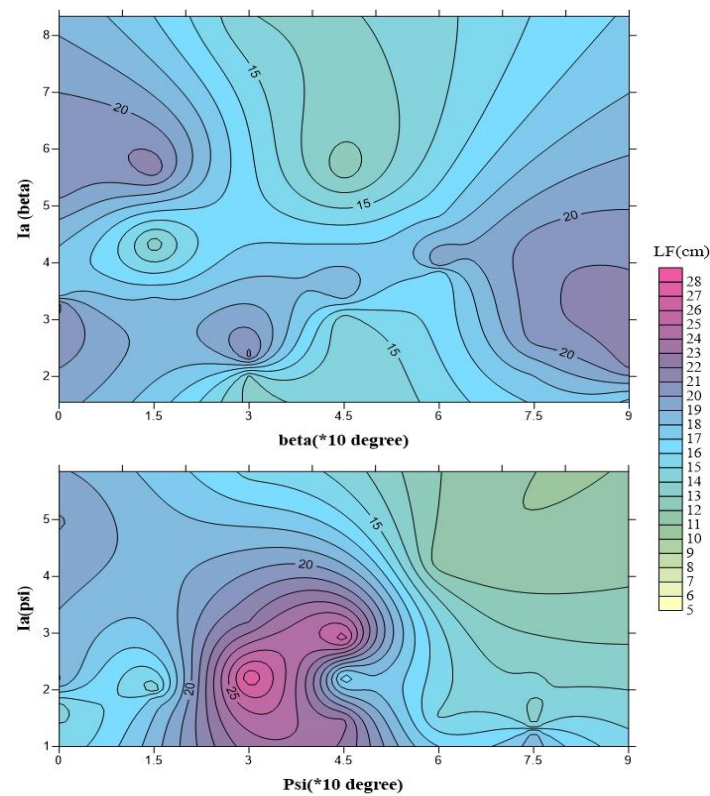


Figure 5. The averages of fracture length (LF) interpolated with Kriging method (Surfer 9): a) based on $Ia_{(\beta)}$ and β and b) $Ia_{(\psi)}$ and ψ .

Conclusions

This experimental study was conducted on the calcareous slate from Arak, Iran. Slate is an anisotropic rock with the tensile strength and fracture pattern considerably affected by the foliation orientation. In Brazilian test, the existence of an anisotropic plane perpendicular to the maximum tensile stresses direction makes a fracture with minimum stresses, because the major failure plane is perpendicular to the maximum tensile stress direction. Hence, the degree of anisotropy has a strong influence on the peak strength measured in the Brazilian test. An average of tensile strength (σ_t) and strength anisotropy index (I_a) have demonstrated that the influence of orientation angle (ψ) is much larger than that of foliation-loading angle (β).

The average value of the failure strength of the three stations varies from 3.21 MPa to 20.94 MPa. The maximum range of tensile strengths and fracture patterns for different β values was within a range of $15^\circ < \psi < 75^\circ$. Moreover, a direct relation was found between the average minimum tensile strength ($\sigma_{t,min}$) and the dry density. It was also identified that the influence of density on minimum tensile strength is more than that of maximum tensile strength. In this connection regard, by increasing the density, the difference between the minimum and maximum tensile strength was reduced. Based on the comparison between data of dry and saturation conditions of Brazilian test, Brazilian tensile strength in the saturated state was averagely 30.8% less than that of the dry state.

The results revealed that the change in the pattern of fractures and fracture length is similar for $0^\circ \leq \psi \leq 15^\circ$ and $75^\circ \leq \psi \leq 90^\circ$. It must be noted that, typically, even in anisotropic rocks such as slates, in the presence of joints and veins? they control the fracture pattern in rocks.

References

1. Ajalloeian R., Lashkaripour G. R., "Strength anisotropies in mudrocks", Journal of Bulletin of Engineering Geology and the Environment, Vol. 59 (2002) 195-199.
2. Anon, "Classification of rocks and soils for engineering geological mapping", Part 1: Rock and soil materials, Bulletin International Association Engineering Geology, Vol. 19 (1979) 355-371.
3. Cárdenes V., Rubio-Ordóñez A., López-Munguira A., et al., "Mineralogy and modulus of rupture of roofing slate: Applications in the prospection and quarrying of slate deposits", Journal of Engineering Geology, Vol. 114 (2010) 191-197.
4. Chen C. S., Pan P., Amadei B., "Determination of Deformability and Tensile Strength of Anisotropic Rock Using Brazilian Tests", Int. J. Rock Mech. & Min. SCI, Vol. 35 (1998) 43-61.
5. Cho J. W., Kim H., Jeon S., Min K.B., "Deformation and strength anisotropy of Asan gneiss, Boryeong shale and Yeoncheon schis", International Journal of Rock Mechanics & Mining Sciences, Vol. 50 (2012) 158-169.

6. Dan D. Q., Konietzky H., Herbst M., "Brazilian tensile strength tests on some anisotropic rocks", *International Journal of Rock Mechanics & Mining Sciences*, Vol.58 (2013)1-7.
7. Debecker B., Vervoort A., "Two-dimensional discrete element simulations of the fracture behavior of slate", *International Journal of Rock Mechanics & Mining Sciences*, Vol. 61(2013) 161-170.
8. Diamantis K., Gartzos E., Migiros G., "Influence of petrographic characteristics on physico-mechanical properties of ultrabasic rocks from central Greece", *Journal of Bulletin of Engineering Geology and the Environment*, Vol.73 (2014) 1273-1292.
9. Duan K., Kwok C. Y., "Discrete element modeling of anisotropic rock under Brazilian test conditions", *International Journal of Rock Mechanics & Mining Sciences* 78 (2015) 46-56.
10. Hudson J. A., Harrison J. P., "Engineering rock mechanics an, introduction to the principles", Published by Elsevier Science Ltd, Pergamon (1997) 444.
11. Heng S., Guo Y., Yang Ch., et al., "Experimental and theoretical study of the anisotropic properties of shale", *International Journal of Rock Mechanics & Mining Sciences*, Vol. 74 (2015) 58-68.
12. Ikari M. J., Niemeijer A.R., Marone C., "Experimental investigation of incipient shear failure in foliated rock", *Journal of Structural Geology*, Vol.77 (2015) 82-91.
13. Islam M. D. A., Skalle P., "An Experimental Investigation of Shale Mechanical Properties Through Drained and Undrained Test Mechanisms", *Journal of Rock Mechanics Engineering*, Vol.46 (2013) 1391-1413.

14. Khanlari G. R., Heidari M., Sepahigero A. A., Fereidooni D., "Quantification of strength anisotropy of metamorphic rocks of the Hamedan province, Iran, as determined from cylindrical punch, point load and Brazilian tests", *Journal of Engineering Geology* 169 (2014) 80-90.
15. Nasserli M. H., Rao K. S., Ramamurthy T., "Failure mechanism in schistose rocks". *International Journal of Rock Mechanics & Mining Sciences*, Vol. 34 (1997) 3-4 (No. 219).
16. Park B., Min K. B., "Bonded-particle discrete element modeling of mechanical behavior of transversely isotropic rock", *International Journal of Rock Mechanics & Mining Sciences*, Vol. 76 (2015) 243-255.
17. Saeidi O., Rasouli V., Geranmayeh Vaneghi R., Gholami R., Torabi, S. R., "A modified failure criterion for transversely isotropic rocks", *Geoscience Frontiers Journal*, Vol.5 (2014) 215-225.
18. Shuai H., Yingtong G., Chunhe Y., Daemen J. K., Zhi L., "Experimental and theoretical study of the anisotropic properties of shale", *International Journal of Rock Mechanics & Mining Sciences*, Vol.74 (2015) 58-68.
19. Siegesmund S., Dürrast H., "Mechanical and physical properties of rocks. In: S. Siegesmund & R. Snethlage", *Journal of Stone in Architecture*, Springer-Verlag Berlin Heidelberg (2011) 97-225, doi: 10.1007/978-3-642-14475-2-3.
20. Smith M. R. (ed), "Stone: Building stone, rock fill and armourstone in construction Geological Society", *Engineering Geology Special Publications*, London (1999) doi:10.1144/ GSL.ENG. 1999.016.01.14.
21. Stoeckhert F., Molenda M., Brenne S., Alber M., "Fracture propagation in sandstone and slate e Laboratory experiments, acoustic emissions and

- fracture mechanics", *Journal of Rock Mechanics and Geotechnical Engineering*, Vol.7 (2015) 237-249.
22. Strohmeyer D., Siegesmund S., "Anisotropic technical properties of building stones and their development due to fabric changes. In: Siegesmund S, Vollbrecht A, Weiss T (eds). *Natural stone, Weathering phenomena, conservation strategias and case studies*. Geological society", London, Special publication, (2002) 205, 115-135.
23. Tavallali A., Vervoort A., "Behavior of layered sandstone under Brazilian test conditions: Layer orientation and shape effects", *Journal of Rock Mechanics and Geotechnical Engineering*, Vol.5 (2013) 366-377
24. Vervoort A., Ki-Bok M., Heinz K., et al., "Failure of transversely isotropic rock under Brazilian test conditions", *Int. J. Rock Mech. & Min. SCI*, Vol. 70 (2014) 343-352.
25. Yavuz Celik M., Ergul A., "The influence of the water saturation on the strength of volcanic tuffs used as building stones. *Environ Earth Sci.*, Vol.74 (2015) 3223-3239.
26. Yilmaz I., Yucel Ö., "Use of the core strangle test for determining strength anisotropy of rocks", *Int. J. Rock Mech. & Min. SCI*, Vol. 66 (2014) 57-63.
27. Zhong J., Liu S., Ma Y., et al., "Macro-fracture mode and micro-fracture mechanism of shale", *Journal of Petroleum Exploration and Development*, Vol.42 (2015) 269-276.